

Comparison of molecular tagging velocimetry data and direct simulation Monte Carlo simulations in supersonic micro jet flows

W.R. Lempert, M. Boehm, N. Jiang, S. Gimelshein, D. Levin

403

Abstract We present results of a combined experimental computational study of free jet flow produced by a 1 mm (height)×5 mm (span) nominally Mach 2 supersonic jet. Two-dimensional maps of u_x , the component of velocity parallel to the principal flow axis, are obtained experimentally, by acetone molecular tagging velocimetry (MTV), and computationally, by the direct simulation Monte Carlo (DSMC) method, at a stagnation pressure and temperature of 10 torr and 300 K, respectively. In all cases, direct comparison of the experimental data and the predictions from DSMC showed excellent agreement, with only minor deviations which, in most cases, can be ascribed to either the inherent uncertainty in the MTV or small uncertainties in the measured wall pressures.

1 Introduction and background

In recent years, the interest in micro devices and systems has increased rapidly, and this trend is expected to continue for years to come. Gaseous flow through and within such devices is a principal consideration in many applications and its understanding can be crucial for optimization of performance. While the last 10 years has seen enormous progress in the general areas of Micro Electro Mechanical Systems (MEMS) design and fabrication,

detailed understanding of fundamental physical processes on these small scales is hampered by the lack of suitable quantitative measurement and simulation tools. In this paper, we present the results of a combined experimental–computational study of the flow produced by a millimeter scale supersonic, Mach 2 micro-jet at low ($Re \sim 3–30$) Reynolds number. The work is primarily motivated by the current interest in micropropulsion systems, such as those which would be used for small satellite orbit maintenance. For example, it has been estimated that for so-called micro-spacecraft, with a total mass in the range 10–100 kg, typical maneuvers would require thrust on the order of 1–10 mN (Ivanov et al. 1999). As pointed out by Ketsdever (2000), system issues dictate that such systems will likely be constrained to operate a low stagnation pressure (of order 10 torr or less), resulting in a device which would inherently operate at low Reynolds number (of order 10 or less). The accompanying viscous loss in propulsion efficiency, defined as the ratio of realized thrust to that corresponding to inviscid flow, is recognized as a major concern (Ketsdever et al. 2001). Clearly, accurate quantitative knowledge of the flow field would provide an important tool for performance optimization, as well as for addressing system integration issues. While there have been several recent computational studies of the flow field produced by such low Reynolds number devices (Alexeenko et al. 2002a, 2002b, Ivanov et al. 1999), there have been, to our knowledge, no corresponding experimental techniques which have been demonstrated to provide the capability to resolve the velocity field produced by such small-scale, low-density, supersonic flow devices. In this paper, we present a direct comparison between experimental microjet velocity data, obtained using acetone molecular tagging velocimetry (MTV) (Lempert et al. 2002a; 2002b) and numerical results obtained using the SMILE computational tool (Ivanov et al. 1998) based on the direct simulation Monte Carlo (DSMC) method (Bird 1994).

MTV is a “time-of-flight” technique in which a laser is used to “write” a line (or set of lines) into a flow by means of an optical resonance with a suitable target tracer molecule (Hiller et al. 1984, Stier and Koochesfahani 1999). We have recently presented a simple MTV approach, which relies on acetone as a molecular tracer (Lempert et al. 2001a). While acetone’s use as a tracer for scalar mixing studies is well understood (Thurber et al. 1998), its application as a velocity tracer is still being explored. Acetone photo-physics is similar in many respects to that of the more commonly employed biacetyl molecule, except

Received: 22 April 2002 / Accepted: 6 November 2002
Published online: 1 February 2003
© Springer-Verlag 2003

W.R. Lempert (✉), M. Boehm, N. Jiang
Department of Mechanical Engineering, The Ohio State University,
Columbus, OH, 43210, USA
E-mail: lempert.1@osu.edu

S. Gimelshein, D. Levin
Department of Aerospace Engineering, The Pennsylvania State
University, University Park, PA, 16802, USA

The authors wish to acknowledge M. Samimy for assistance with the nozzle design and for many helpful discussions. The assistance of S. Sethuram with nozzle fabrications is also acknowledged. W. Lempert, M. Boehm, and N. Jiang wish to acknowledge the support of the US Air Force Office of Scientific Research programs in Turbulence and Rotating Flows (T. Beutner technical monitor), and Space Propulsion and Power (M. Birkan technical monitor). Support was provided for S. Gimelshein and D. Levin under the US Army ARO Grant number DAAD19-02-1-0196 in support of the Innovative Science and Technology Office of MDA.

that it is excited in the wavelength range of approximately 230–340 nm. This provides a convenient match to the outputs of either the Nd:YAG (fourth harmonic at 266 nm) or XeCl (309 nm) lasers. However, as will be discussed in more detail below, it appears that under certain conditions, acetone is readily photo-dissociated, forming CH radicals, which can be used advantageously.

MTV is similar, in many respects, to what is termed “flow tagging velocimetry.” Flow tagging utilizes a pair of excitation lasers, one of which “tags” the flow by optically driving a fraction of the molecules into an excited, metastable electronic and/or vibrational state, or inducing a photochemical reaction. After a suitable time delay, standard planar laser fluorescence imaging techniques, employing a second laser, are used to “interrogate” the displacement of the initially tagged fluid elements. Gas-phase oxygen and ozone-based flow tagging have recently been reviewed by Miles et al. (2000) and Pitz et al. (2000), respectively. Application of MTV to incompressible flow has recently been reviewed by Koochesfahani et al. (2000), who employed long-lifetime supramolecules, and Lempert and Harris (2000), who employed caged dye photo-activated fluorophores.

In previous work, we have demonstrated the potential of the MTV technique for supersonic micro jet flow by performing proof of concept measurements of the flow produced by a 1-mm-diameter, circular nozzle, at static pressures in the range 1–40 torr. In this paper, we present new experimental and computational results, focusing on the free jet flow field produced by a two-dimensional nominally Mach 2 nozzle with exit dimensions 1 mm (height)×5 mm (span), operated with a stagnation pressure of 10 torr. The system Mach number and geometry were chosen in order to provide a model baseline system with thrust of order mN, which was readily fabricated and which produced a supersonic flow which was neither trivial nor exceedingly complex. (It was not intended to replicate an actual micropropulsion device.) Experimental and DSMC two-dimensional spatial profiles of u_x , the component of velocity parallel to the principal flow axis, are obtained for both near pressure matched and highly underexpanded conditions. The particular emphasis of the work is to: (i) demonstrate the absolute accuracy of the MTV method by providing quantitative comparison of the experimental and computational data, and (ii) demonstrate the extension of the MTV diagnostic for application to supersonic, micron-scale flow fields with sub-torr static pressure, such as the plume of an underexpanded microthruster.

The DSMC method is chosen in this work as the principal numerical tool because of its established ability to reliably predict low-density flows. Work has been performed by different research groups on the DSMC modeling of cold gas flows in MEMS devices, primarily concentrating on axisymmetric micronozzles. Recently, the method was used to model three-dimensional micronozzles (Alexeenko et al. 2002a, 2002b). The work described in Alexeenko et al. (2002a) was aimed at the numerical study of viscous effects in micronozzles and a comparison of different geometric configurations, axisymmetric and three-dimensional, in terms of thrust

performance and flow fields. A subsequent paper (Alexeenko et al. 2000b) on micronozzles dealt with heated and high-temperature flows in axisymmetric and three-dimensional nozzle configurations. Note that the comparison of the DSMC results with the measured values of the total impulse flux (Alexeenko et al. 2002a, 2002b) have shown good agreement between the experimental and numerical data.

2 Experimental/computational techniques

2.1 Experimental

MTV images were obtained from the flow produced by a 1 mm (height)×5 mm (span) contoured nozzle, which was designed using the method of characteristics to produce an exit Mach number of 2, assuming inviscid flow. The flow facility and optical diagnostics have been described in detail previously (Lempert et al. 2002a, 2002b), and will, therefore, only be summarized here. The nozzle, illustrated in Fig. 1, is fabricated using electric discharge machining, based on an approach described by Bayt and Breuer (2001). Other major elements of the facility include an acetone vapor seeding chamber, a 1,000 liter/min rotary pump, and a 25 mm (height)×25 mm (span)×100 mm (length) optical access enclosure. By suitable combination of stagnation pressure, flow rate, and pumping speed, the nozzle can be operated in flow regimes ranging from pressure matched ($P_{\text{exit}}=P_{\text{ambient}}$) to highly underexpanded ($P_{\text{exit}}\sim 5\text{--}10P_{\text{ambient}}$). Static pressure is measured using three Baratron pressure gauges with taps located in the nozzle plenum, in a straight section ~ 1 mm upstream of the nozzle exit, and in the flow enclosure. For all the data to be presented in this paper, the facility was operated with a stagnation pressure of 10 torr. Ambient background pressure varied between 0.40 torr (the lowest achievable at $P_0=10$ torr with our modest vacuum system) and ~ 3 torr, which corresponds to approximately perfect (“pressure matched”) expansion. Figure 2 shows the measured ratio of stagnation pressure to nozzle exit pressure as a function

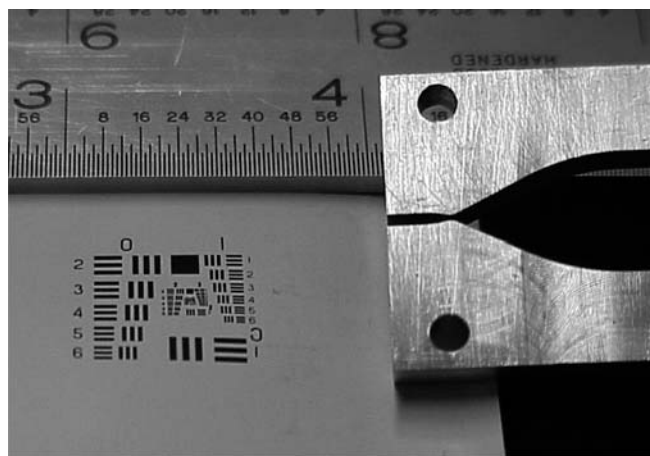


Fig. 1. Photograph of Mach 2 nozzle prior to attachment of top and bottom walls. Plenum is on the right. Scale is in inches

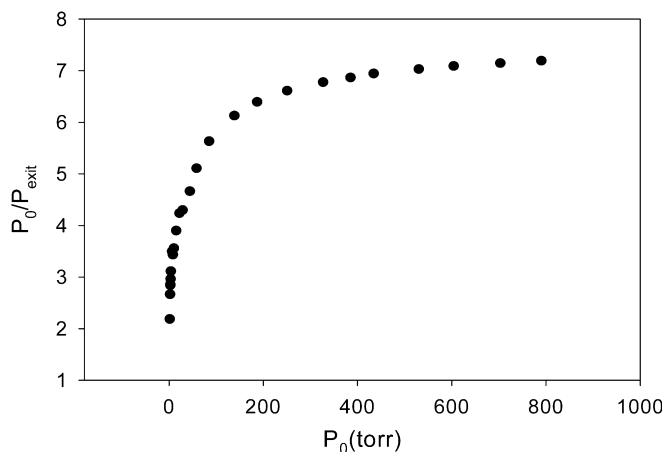


Fig. 2. Experimental ratio of stagnation pressure to nozzle exit pressure as a function of stagnation pressure for 1×5-mm nominally Mach 2 rectangular nozzle

of stagnation pressure when the facility is operated at its maximum pumping speed. It can be seen that the pressure ratio increases rapidly as the stagnation pressure is increased from approximately 10 to 50 torr, after which it continues to rise more slowly, leveling off to a ratio of ~ 7.1 . This corresponds, assuming isentropic flow at $T_0=300$ K, to a Mach number of 1.94.

The tagging laser beam was incident to the flow in a direction parallel to the height (short axis) dimension. Single lines were written on the spanwise centerline at locations ranging from ~ 0.1 mm (0.1 h) to 5 mm (5 h), where h is the height of the nozzle, from the nozzle exit by focusing ~ 5 mJ of the fourth harmonic output (at 266 nm) from a pulsed Nd:YAG “mini” laser using a 100-mm focal length plano-convex lens. Displaced images were captured using an 18-mm micro-channel plate intensified ICCD camera, employing an optical system with ~ 4 :1 image magnification, resulting in an object plane resolution of ~ 10 – 20 microns and a spatial scale of ~ 10 microns/pixel. The intensifier gate width was 20 ns, and the time delay between tag and interrogation varied between 200 and 500 ns. Images were averaged (on the CCD) for approximately 3–10 s, at a laser repetition rate of 10 Hz, prior to read out.

Velocity was extracted from pairs (t_0 and displaced) of MTV images using an in-house, PC-based image-processing code which employs standard least-squares fitting techniques following the method described by Bevington (1969). From each image (i.e., single MTV line), a set of approximately 300 individual “slices” of data, corresponding to height above/below the nozzle centerline, is extracted and digitized, forming a two-dimensional (height×displacement) array of grey-scale intensity values. Displacement is determined by least-squares fit of the intensity to an assumed Gaussian spatial profile. u_x is defined as the displacement divided by the elapsed time. Previous measurements (Lempert et al. 2002a, 2002b) have demonstrated u_x velocity precision of ± 610 m/s (2σ) for static pressure in the range 1–40 torr. However, as will be described in detail below, the majority of the MTV measurements presented in this paper are performed at significantly lower static densities, resulting in reduced precision.

2.2

Computational

The DSMC method is used in the computations of the nozzle flow. Being applied to the problem under consideration, the DSMC method has several important advantages. This approach takes into account viscosity, and the finite thickness of the Knudsen layers and shock waves is physically grounded. The development of fast computers and parallel algorithms allows one to use the DSMC method for computing flows with Knudsen numbers as low as $Kn \sim 0.001$, and, as such, this method has become a powerful tool for modeling near-continuum flows. The DSMC-based computational tool SMILE (Ivanov et al. 1998; Alexeenko et al. 2002a) is used in this study. Collisions are modeled using the majorant frequency scheme. Rectangular adaptive grids were used for collisions and macroparameter sampling. The cell size for the collision grid depends on the local mean free path. The variable hard sphere model was used for the molecular potential. The energy exchange between the translational and rotational modes follows the Larsen–Borgnakke model with the temperature-dependent rotational relaxation number. The number of simulated molecules was about 15 million, and the number of collisions cells was about 3 million.

3

Results and discussion

3.1

Experimental accuracy

Velocity accuracy for the MTV technique has been discussed in detail previously (Lempert et al. 2002b). Fundamentally, the accuracy of any Lagrangian reference frame-based optical velocimetry method is dictated by the accuracy with which the centroid of fluid displacement can be located from a digitized image of optical intensity. For the plume of an underexpanded, even moderately supersonic jet, of order 10 torr stagnation pressure, even the near field will rapidly expand to static pressure of less than 1 torr. Such measurements, presented below, represent a significant “pushing” of the measurement technique due to the combination of low static pressure and large streamwise velocity gradient. The low pressure affects the measurements in two ways. First, the number density of tracer molecules is quite low, so the signal is inherently limited. Additionally, and very significantly, mass diffusion causes substantial broadening of the interrogated line profiles. Figure 3 shows three sets of “slices” of grey-scale intensity, and corresponding least-squares fits, taken from the flow centerline of interrogated MTV images obtained 1.0 mm, 3.0 mm, and 4.4 mm downstream from the nozzle exit for the case $P_0=10$ torr, $P_{\text{exit}}=0.87$ torr and $P_{\text{ambient}}=0.40$ torr, which is the most highly underexpanded case studied (see Fig. 13, which will be described in more detail in the next section). The centerline static pressures at the 1.0, 3.0, and 4.4 mm downstream locations, determined from the DSMC simulation, are ~ 0.60 , 0.30, and 0.10 torr, respectively. In each case, the data and fit which contains the leftmost peak is obtained from MTV images taken at very short time delay (30 ns), whereas the rightmost data and fit correspond to data obtained at

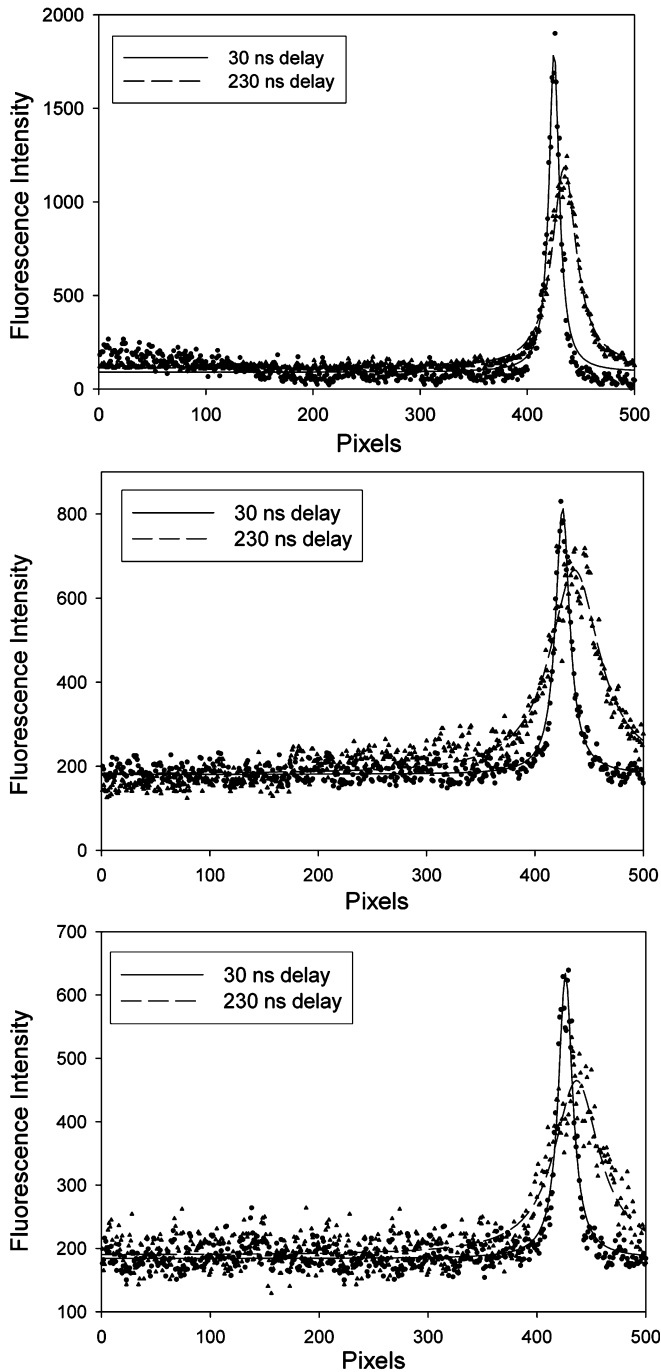


Fig. 3. Representative digitized single slices of MTV data for the most underexpanded case studied ($P_o/P_{\text{exit}}/P_{\text{ambient}}=10.0/2.87/0.40$ torr). Slices taken from the flow centerline at locations 1.0, 3.0, and 4.4 mm (from top to bottom) downstream from the nozzle exit. Corresponding static pressures are 0.60, 0.30, and 0.10 torr, respectively. One pixel corresponds to approximately 10.5 microns

230 ns. The displacement divided by the time difference is defined as u_x . In order to eliminate interferences due to elastic scattering from the nozzle surface and/or short lifetime fluorescence from the enclosure windows, 30 ns is chosen, rather than zero, for the baseline image. Due to potential drifts in the laser tagging and/or imaging optics it is important to take separate baseline data for each velocity measurement. Note that the displaced line, which is

the rightmost, is substantially broadened, relative to the original line, due to rapid mass diffusion. As a general rule of thumb, the center of grey-scale intensity can be determined to $\sim 3\text{--}10\%$ of the *full width* of the profiles, dependent upon the signal to noise ratio. The combination of rapid diffusion and large streamwise velocity gradient dictates that relatively short time delays (order 200 ns) be utilized for the underexpanded flow data. The net result is that the shift to width ratio of the tagged fluid elements is limited to $\sim 25\%$, as can be seen from Fig. 3. This, in combination with the relatively poor signal to noise due to the low tracer density, results in velocity precision, for a single slice of data, of order ± 20 , 50, and 70 m/s (2σ), for the 0.60, 0.30, and 0.10 torr cases, respectively, illustrated in Fig. 3 (top to bottom). Nonetheless, as will be shown in the next section, meaningful MTV data can be obtained, particularly when used in combination with computational predictions.

3.2 Flow field results

Figure 4 shows a collage of individual MTV images obtained at tagging locations varying from 0.10 to ~ 5 mm (or 0.1 \sim 5 h) downstream from the nozzle exit. In this case, the nozzle was operated near pressures matched with the measured stagnation pressure of 10 torr, exit pressure of 3.16 torr, and ambient background pressure of 2.74 torr. The flow is from left to right, and in all cases the time delay between tag and interrogation was 500 ns. Qualitatively, even very close to the nozzle exit, significant curvature is seen throughout the entire horizontal profile in the inter-

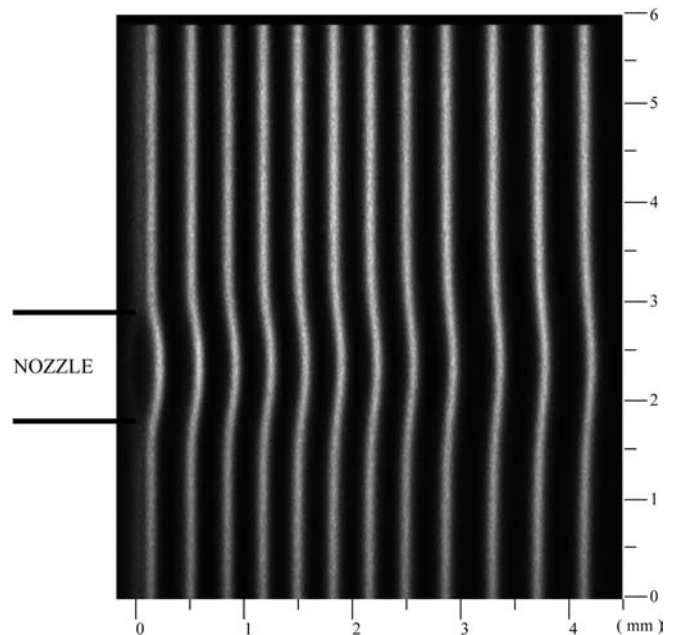


Fig. 4. Representative collage of MTV images obtained from jet produced by nominally Mach 2 nozzle with exit dimensions 1 mm (height) \times 5 mm (span). Flow is approximately pressure matched with $P_o=10$ torr, $P_{\text{exit}}=3.16$ torr, and $P_{\text{ambient}}=2.74$ torr. Flow is from left to right and tagging positions range from 0.1 to ~ 5 mm downstream of nozzle. Time delay between tagging and interrogation is 500 ns (for clarity, not all images obtained are shown)

rogated images, implying a complete lack of inviscid "core" flow within the nozzle. Further evidence for this conclusion is given in Fig. 5, which shows the DSMC prediction for the u_x profile at the nozzle exit. Note, that even on the centerline, the DSMC simulation predicts a flow velocity of ~ 375 m/s, as compared to the isentropic value of 509 m/s. Also, while not indicated in the figure, the DSMC predicts the density on centerline to be 5.5×10^{-3} kg/m³, as opposed to the isentropic value of 3.81×10^{-3} kg/m³, for Mach 1.94 flow with P_0 and T_0 equal to 10 torr and 300 K, respectively. Since the dynamic pressure scales as ρu_x^2 , this corresponds to a viscous loss in dynamic pressure of $\sim 22\%$ (775 N/m² as opposed to 985 N/m²). Figure 6 shows experimental centerline velocity data from the images in Fig. 4. It can be seen, as expected for this nearly perfectly expanded case, that the centerline velocity is approximately constant as a function of downstream distance. However, the centerline velocity of ~ 344 m/s corresponds, assuming isentropic flow, to an exit Mach number of only ~ 1.10 . This is additional experimental evidence of the significant boundary layer growth within the nozzle under these conditions. (Note that the experimental exit pressure, 3.16 torr, is slightly higher than that assumed for the simulation, 2.87 torr, which most likely explains the lower experimental velocity value).

Figure 7a, b shows two-dimensional maps of u_x obtained from DSMC (a) and from the MTV measurements (b) corresponding to the grey scale image data of Fig. 4.

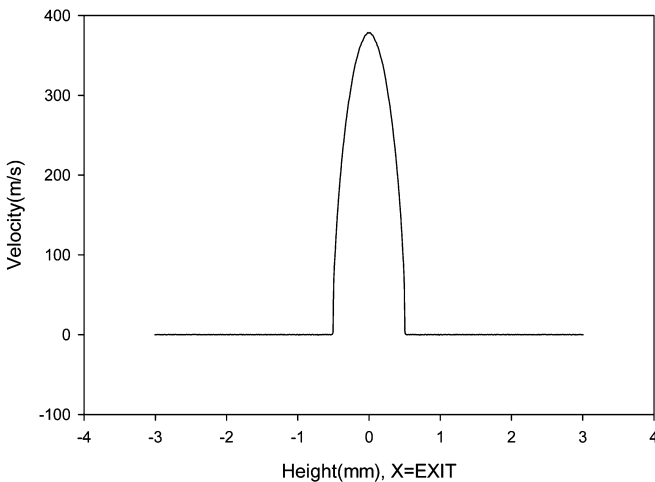


Fig. 5. DSMC u_x profile at nozzle exit

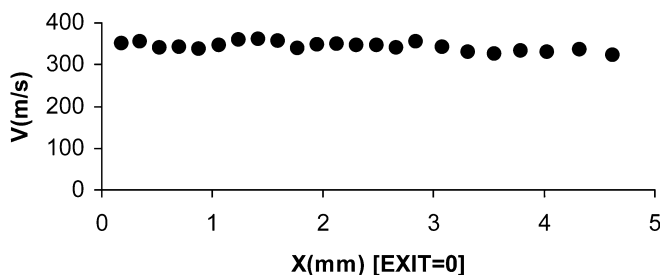


Fig. 6. Experimental centerline velocity data obtained from the images in Fig. 4

Note, however, that the DSMC simulation assumes a perfect expansion, with ambient back pressure precisely equal to the exit pressure. As in Fig. 8, the horizontal/vertical axes represent downstream location and height, respectively (both in mm). It should also be noted that for the DSMC case the origin of the vertical axis is defined as the flow centerline, whereas for the MTV data, the vertical origin is arbitrary. It is evident from inspection of color plates a and b that the DSMC simulation has reproduced the experimental flow field with a high degree of accuracy. This can be seen even more quantitatively in Fig. 7, which shows a direct comparison of experimental and DSMC horizontal velocity profiles at the 0.5, 1.0, and 4.0 mm downstream locations. Note that the DSMC data have not been scaled or fitted in any way to reproduce the experimental results. In fact, both the experimental and DSMC data were obtained completely independently, with the results simply overlaid on top of one another. With the exception of the slightly reversed flow (i.e., negative u_x) predicted by the DSMC in the outer region of the shear layer at the most downstream location and the slightly sharper experimental profiles, the absolute agreement is clearly quite good.

Figure 7c, d is similar to a, b except that, in this case, the nozzle was operated underexpanded, with a stagnation pressure of 10 torr, exit pressure of 2.87 torr, and ambient background pressure of 0.87 torr. The rapid expansion characteristic of such an underexpanded jet is clearly evident in both figures, as is the weak shock located at approximately 4 mm (4 h) downstream from the exit.

Figure 9, which is similar to Fig. 8, shows horizontal velocity profiles at the 0.65, 1.1, and 4.1 mm downstream locations. The more "flat-topped" nature of the velocity profile in the near field of the jet is clearly evident. Once again, at the far downfield location, the DSMC predicts a very small reverse flow, as well as a higher centerline velocity. With the exception of this and a slightly narrower ($\sim 3\%$) experimental profile at the 1.1 mm downstream location, the agreement is again quite good. As an additional comparison for this underexpanded case, Fig. 10 shows a comparison of centerline MTV velocity data with DSMC predictions. Note that reduction of the ambient back pressure, which would more closely mimic the operation of an actual device, results in a not insignificant increase in the predicted centerline exit velocity to ~ 420 m/s, compared to the pressure-matched value of ~ 375 m/s. Clearly, while somewhat lower, the viscous loss in dynamic pressure is still considerable. In addition, a slight asymmetry is evident in the experimental data in the vicinity of the maximum velocity, which does not appear in the simulation. Finally, the location of the minimum experimental value of u_x is displaced slightly downstream with respect to the DSMC, and the local minimum in the experimental velocity is greater. However, as shown below, the flow expansion is extremely sensitive to the ambient pressure, so that these discrepancies may be attributable to a slight inaccuracy in the experimentally measured values of wall pressure.

In an attempt to assess this hypothesis, data were taken at an even lower ambient back pressure. Figure 11 shows a collage of MTV lines which were obtained under condi-

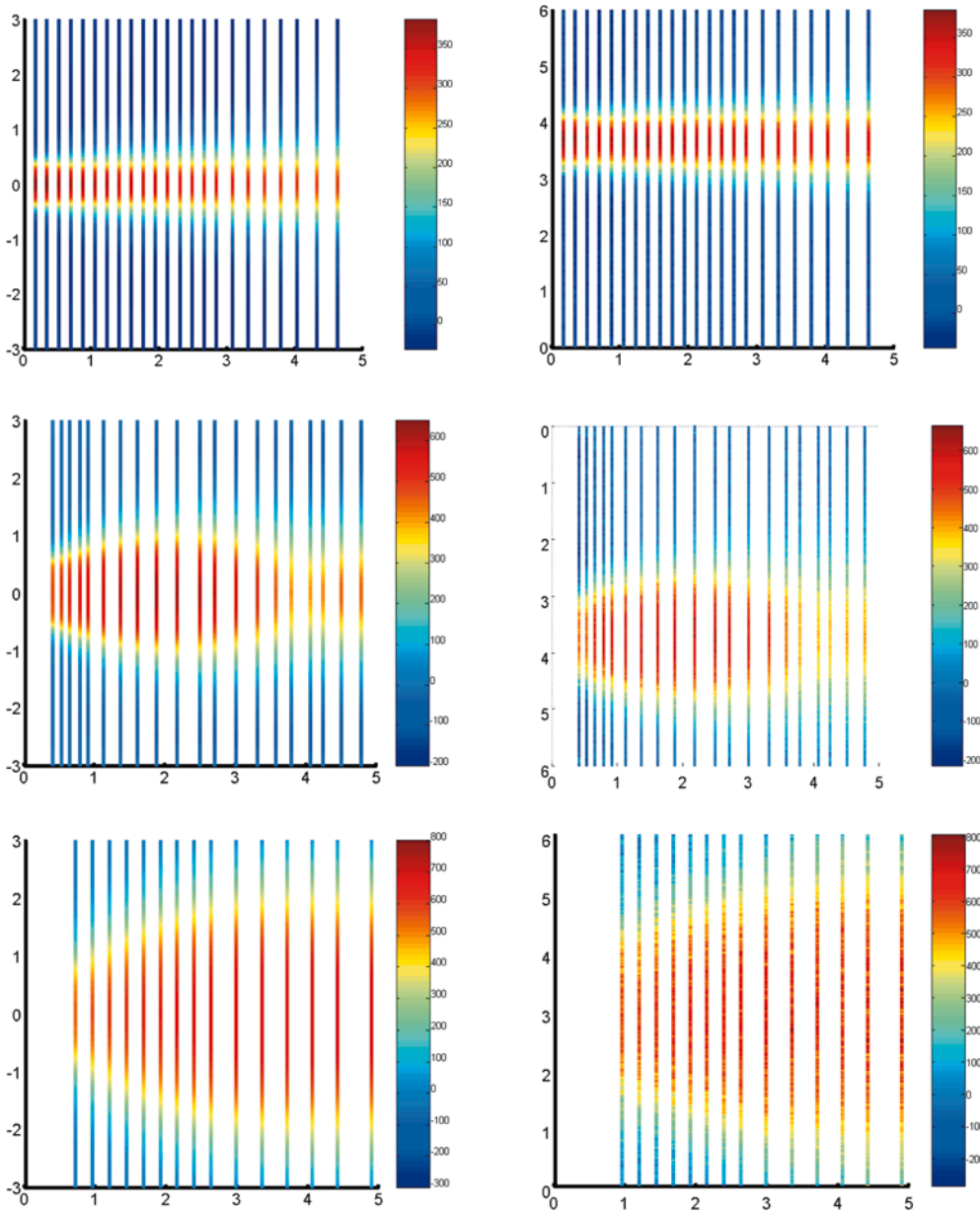


Fig. 7a-f. a, b (left/right) u_x maps for $P_0=10$ torr, $P_{\text{exit}}=2.87$ torr, $P_{\text{ambient}}=2.87$ torr (DSMC left) and $P_0=10$ torr, $P_{\text{exit}}=3.14$ torr, $P_{\text{ambient}}=2.87$ torr (Expt right); c, d U_x maps for $P_0=10$ torr, $P_{\text{exit}}=2.87$ torr, $P_{\text{ambient}}=0.87$ torr (DSMC left; Expt right); e, f u_x maps for $P_0=10$ torr, $P_{\text{exit}}=2.89$ torr, $P_{\text{ambient}}=0.4$ torr (DSMC left; Expt right)

tions identical to that of Fig. 7c, d except that the ambient backing pressure was further reduced to 0.40 torr (the limit of the pumping system). It is found that this relatively small change in back pressure significantly affects the flow field, producing a significantly more rapid expansion. This behavior is more readily seen from inspection of the two-dimensional velocity profiles given in the color plates in Fig. 7e, f. Once again, the overall agreement between the MTV data and the DSMC simulation is extremely good. Figure 12 shows the centerline MTV and DSMC data, similar to those of Fig. 10. Once again, it can be seen that the DSMC predicts a centerline value of u_x at the exit equal to ~ 420 m/s, essentially unchanged from that for the 0.87 torr back pressure case. Also, while the agreement between the DSMC and data is quite good in the near to intermediate field, there is clearly a larger discrepancy beyond ~ 4 mm downstream. It is stressed, however, that, as illustrated in Fig. 3, the precision of the

data obtained at these very low static pressure conditions (~ 0.10 torr) is relatively poor (± 50 – 70 m/s). In this regard, it should also be noted that, while it is not obvious from the MTV images shown in Fig. 10, for this case we were unable to extract reliable velocity data for images obtained less than 1 mm downstream from the nozzle exit, due to stray light interference from nozzle scattering. A better means of comparison is illustrated in Fig. 13, which gives horizontal velocity profiles at the 1.0, 3.0, and 4.4 mm downstream locations. From Fig. 13 it can be seen that, while the scatter is relatively high, the overall level of agreement between the data and DSMC is, again, quite good. At the 3.0 and 4.4 mm downstream positions, the data do appear to be somewhat systematically low in the vicinity of the centerline, but additional measurements are clearly required to determine whether this result is real. In particular, it should again be noted that the flow field is quite dependent upon ambient pressure, and the

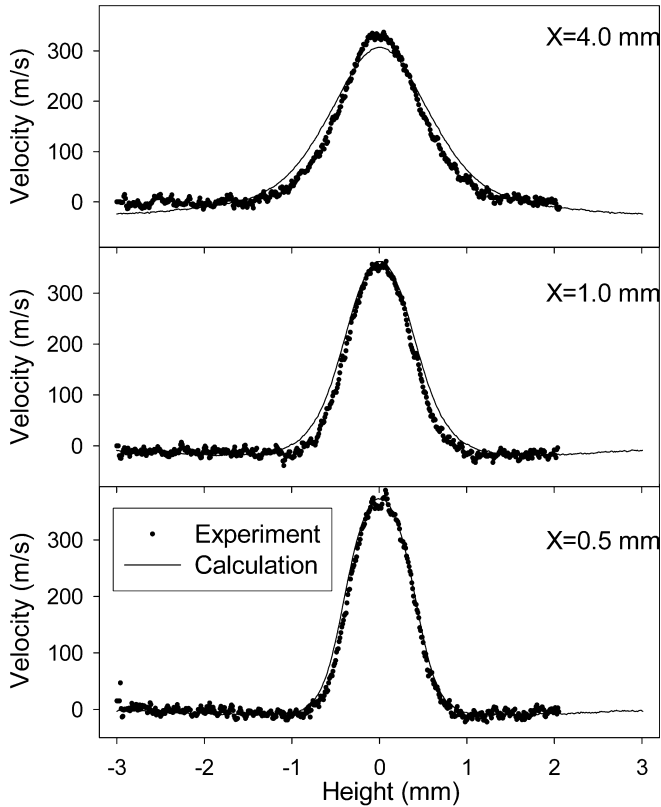


Fig. 8. Comparison of experimental and DSMC horizontal velocity profiles for near pressure-matched flow ($P_o/P_{\text{exit}}/P_{\text{ambient}}=10.0/3.16/2.74$ torr, respectively), at 0.50, 1.0, and 4.0 h downstream from nozzle exit

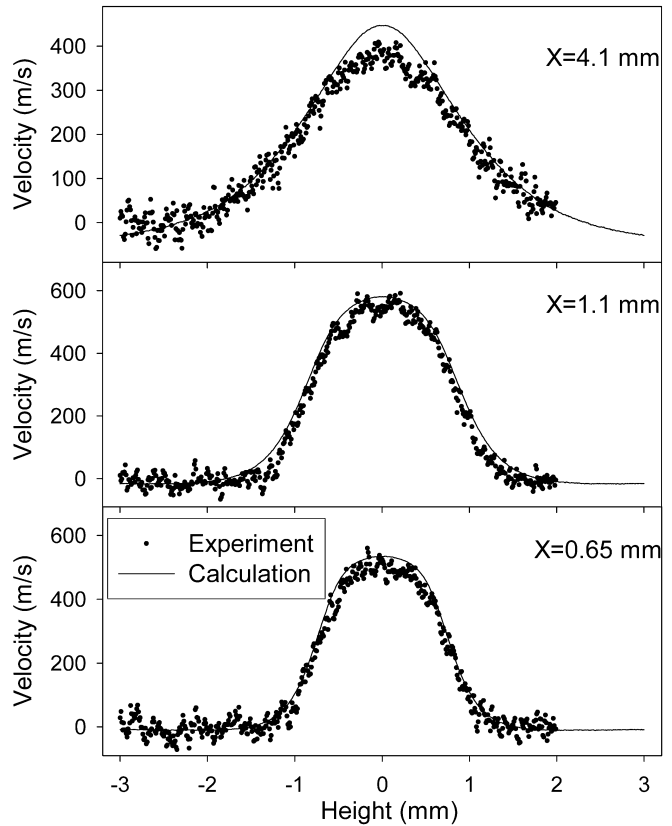


Fig. 9. Comparison of experimental and DSMC horizontal velocity profiles for underexpanded case ($P_o/P_{\text{exit}}/P_{\text{ambient}}=10.0/2.87/0.87$ torr, respectively), at 0.65, 1.1, and 4.1 h downstream from nozzle exit

discrepancy may also be due to uncertainty in the measured wall pressure values. Finally, there appears to be a discontinuity in the measured value of u_x in the downstream shear layers. The fact that this is observed on both top and bottom and at both the 3.0 and 4.4 mm locations is suggestive that the effect may be real, although it clearly also needs to be confirmed by additional experiments.

For completeness, we mention here that additional MTV data have been obtained from the Mach 2, 1×5-mm nozzle at stagnation pressures of 50 and 150 torr, for both ideally and underexpanded conditions (Lempert et al. 2002a). While quantitative comparisons between theory and experiment have not been performed, the expected trend of increasing centerline u_x and decreasing shear layer thickness with increasing P_o was observed. More quantitatively, for the pressure-matched case at 50 torr ($P_{\text{exit}} \sim 10$ torr), u_x was found to increase to ~ 480 m/s, 95% of the isentropic value, indicating greatly reduced viscous losses in dynamic pressure. For the 150 torr case ($P_{\text{exit}} \sim 26$ torr), u_x was found to be equal to the isentropic value, to within the experimental uncertainty.

4

Acetone fluorescence characteristics

Despite the successful application of the acetone MTV technique, the origin of the relatively long lifetime fluorescence signal, upon which the method is based, is not completely understood. As reported previously (Lempert et al. 2002a), the lifetime of the observed fluorescence

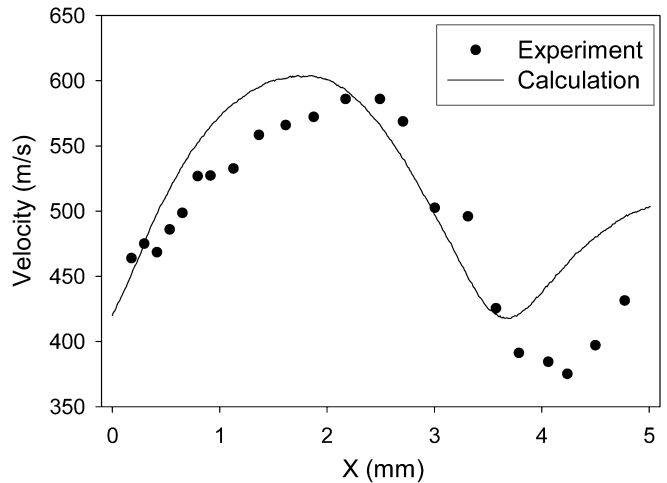


Fig. 10. Comparison of measured and calculated velocity profiles along the nozzle centerline for the underexpanded case $P_o/P_{\text{exit}}/P_{\text{ambient}}=10.0/2.87/0.87$ torr, respectively. $X=0$ corresponds to the nozzle exit

decay (~ 0.10 – $1.0 \mu\text{s}$, depending upon pressure), while much longer than the very rapid decay (~ 4 ns) utilized for scalar mixing studies, is much shorter than the order of millisecond phosphorescence decay reported for biacetyl (Hiller et al. 1984; Stier and Koochesfahani 1999). In the

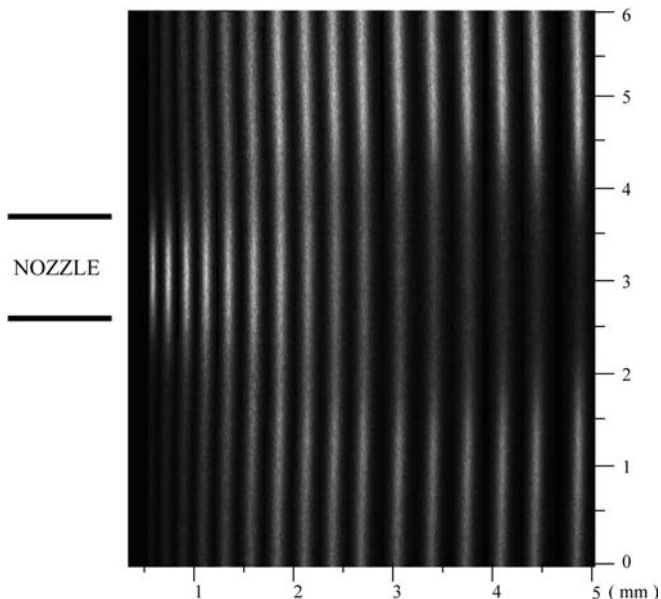


Fig. 11. Collage of MTV images for $P_o/P_{\text{exit}}/P_{\text{ambient}} = 10.0/2.87/0.40$ torr, respectively. Time delay between tag and interrogation is 200 ns

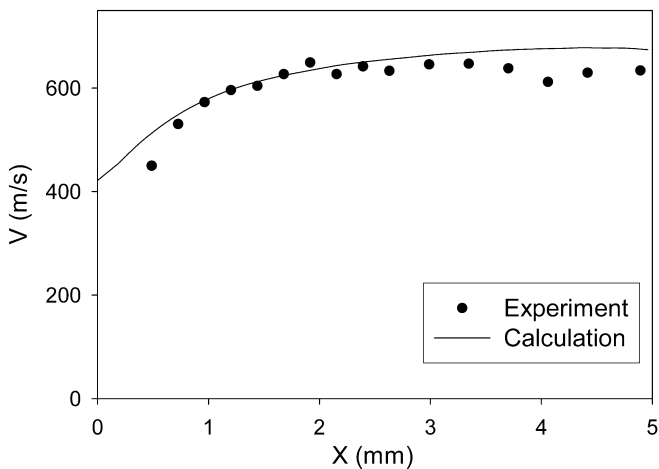


Fig. 12. Centerline MTV and DSMC velocity data corresponding to images of Fig. 11

absence of oxygen, it is a long-lived triplet state, which serves as the basis for biacetyl MTV measurements (Stier and Koochesfahani 1999), a state which is rapidly quenched in the presence of even trace quantities of oxygen. A similar long lifetime triplet state is also known to exist in acetone (Thurber et al. 1998), rapid noncollisional transfer to which serves as the basis for quenching rate independent scalar mixing intensities. However, we have recently shown that MTV images can also be obtained in air flows (Lempert et al. 2001). Clearly, an additional mechanism must be responsible for the MTV signal in these cases. Figure 14 shows preliminary spectrally and temporally resolved emission measurements obtained in acetone seeded air at ~ 20 torr static pressure (Similar spectra were obtained for acetone seeded N_2 flow). The measurements

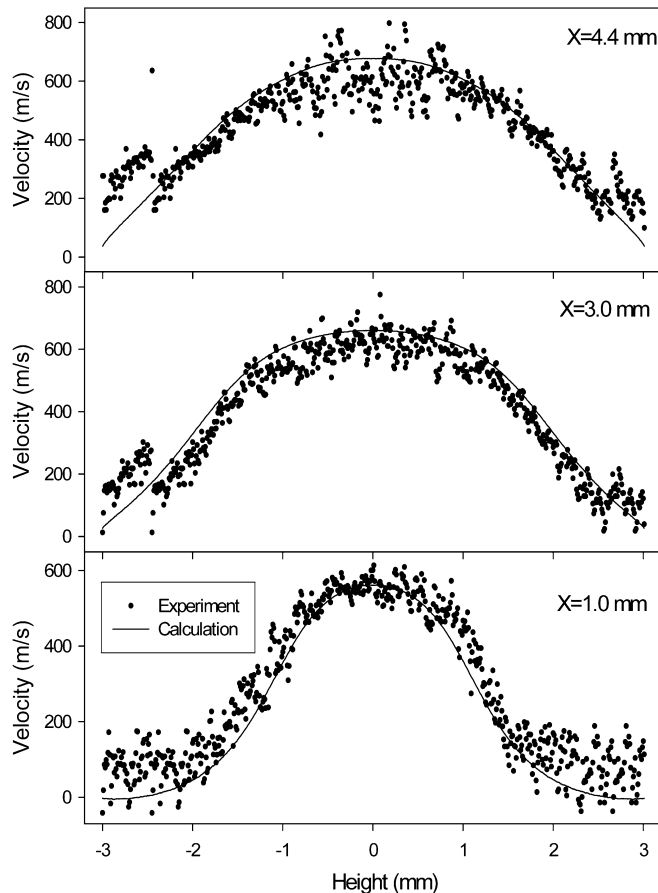


Fig. 13. Comparison of experimental and DSMC horizontal velocity profiles for underexpanded case ($P_o/P_{\text{exit}}/P_{\text{ambient}} = 10.0/2.87/0.40$ torr, respectively), at 1.0, 3.0, and 4.4 h downstream from nozzle exit

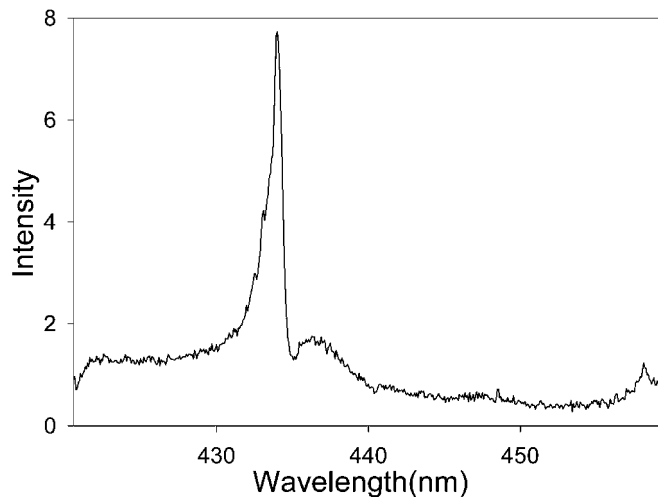


Fig. 14. Emission spectrum in vicinity of 430 nm obtained from acetone seeded air excited by MTV tagging laser at 0.266 microns (acetone seeded N_2 is similar). Spectral signature is characteristic of CH radical

were performed by replacing the ICCD imaging camera with an optical multichannel analyzer (OMA), which used the ICCD camera for detection. Otherwise, the spectral

measurement was the same as the MTV measurement. The asymmetric dual peak feature in the vicinity of 435 nm corresponds to the well-known emission band of the CH radical (Eckbreth 1996), which is perhaps formed in a two-step photolysis sequence:



We intend to explore this in more detail in the near future.

5 Conclusions

The free jet flow field produced by a 1 mm (height) × 5 mm (span) Mach 2 supersonic jet has been studied both experimentally, using acetone MTV, and computationally, by DSMC, at a stagnation pressure and temperature of 10 torr and 300 K, respectively. Quantitative, spatially resolved velocity data were obtained for flow field static pressure as low as approximately 0.10 torr with a spatial resolution of ~20 microns. Least-squares fitting derived statistical uncertainties of ±20, 50, and 70 m/s (2σ) were determined for static pressures of 0.60, 0.20, and 0.10 torr, respectively, for single slices of MTV data. While the statistical uncertainty is somewhat high, this nonetheless represents a significant low pressure extension of the MTV technique and represents the first, to our knowledge, report of quantitative MTV data of any sort at static pressure below 1 torr.

Detailed two-dimensional profiles of u_x , the velocity component parallel to the principal flow axis, have been compared to DSMC predictions for three cases, two underexpanded, and one near pressure matched. The pressure-matched case exhibits significant curvature throughout the profile, indicating a complete lack of inviscid core flow within the nozzle. The centerline value of ρu_x^2 is found to be only approximately 78% of the isentropic value, representing a significant viscous loss in dynamic pressure. For the 0.87 and 0.40 torr back pressure underexpanded cases, while MTV data are not available at the nozzle exit, the DSMC indicates that the centerline velocity increases to ~83% of the isentropic value. These results should be compared with previous work at stagnation pressure of 50 and 150 torr, in which the centerline values of u_x were found to be very close to the isentropic value. For the underexpanded cases, the plume exhibits the expected rapid expansion, and the near field velocity profile becomes significantly more flat-topped. In all cases, agreement between the experimental data and the DSMC predictions was excellent, with only minor deviations which, in most cases, can be ascribed to either the inherent uncertainty in the MTV data at low flow densities or small uncertainties in the measured wall pressures.

Preliminary acetone photo-physics measurements indicate that a substantial fraction of the long lifetime emission which serves as a basis for the MTV technique originates from CH radical, presumably formed by acetone

photolysis. We intend to explore this in more detail in the future.

References

- Alexeenko AA, Collins RJ, Gimelshein SF, Levin DA, Reed BD (2002a) Numerical modeling of axisymmetric and three-dimensional flows in MEMS nozzles. *AIAA J* 40:897–904
- Alexeenko AA, Gimelshein SF, Levin DA, Collins RJ, Markelov GN (2002b) Numerical simulation of high-temperature gas flows in a millimeter-scale thruster. *J Thermophys Heat Transfer* 16:10–16
- Bayt R, Breuer K (2001) Systems design and performance of hot and cold supersonic microjets. *AIAA-2001-0721*, 39th AIAA Aerospace Sciences Meeting, Reno, Nev.
- Bevington, PR (1969) *Data reduction and error analysis for the physical sciences*. McGraw Hill, New York
- Bird GA (1994) *Molecular gas dynamics and the direct simulation of gas flows*. Clarendon Press, Oxford
- Eckbreth AC (1996) *Laser diagnostics for combustion temperature and species*. Gordon & Breach, Amsterdam
- Hiller B, Booman RA, Hassa C, Hanson RK (1984) Velocity visualization in gas flows using laser-induced phosphorescence of biacetyl. *Rev Sci Instrum* 55:1964–1997
- Ivanov MS, Markelov GN, Gimelshein SF (1998) Statistical simulation of reactive rarefied flows: numerical approach and applications. *AIAA-98-2669*
- Ivanov MS, Markelov GB, Ketsdever AD, Wadsworth DC (1999) Numerical study of cold gas micronozzle flows. *AIAA-99-0166*, 37th AIAA Aerospace Sciences Meeting, Reno, Nev.
- Ketsdever AD (2000) System considerations and design options for microspacecraft propulsion systems. In Micci M, Ketsdever AD (eds) *Micropropulsion for small spacecraft*, AIAA Progress Series in Astronautics and Aeronautics, vol 187. AIAA, Reston, Va.
- Ketsdever AD, Green AA, Muntz EP (2001) Momentum flux measurements from under expanded orifices: applications for microspacecraft systems. *AIAA-2001-0502*, 39th AIAA Aerospace Sciences Meeting, Reno, Nev.
- Koochesfahani M, Cohn R, MacKinnon C (2000) Simultaneous whole-field measurements of velocity and concentration fields using a combination of MTV and LIF. *Meas Sci Technol* 11:1289–1300
- Lempert WR, Harris SR (2000) Flow tagging velocimetry using caged dye photo-activated fluorophores. *Meas Sci Technol* 11:1251–1258
- Lempert WR, Jiang N, Sethuram S, Samimy M (2001) Molecular tagging velocimetry measurements in supersonic micro jets. *Proceedings of 2001 ASME International Mechanical Engineering Congress and Exposition*, 11–16 November 2001. ASME, New York
- Lempert WR, Jiang N, Samimy M (2002a) Development of molecular tagging velocimetry for high speed flows in micro systems. *AIAA-2002-0296*, 40th AIAA Aerospace Sciences Meeting, Reno, Nev., 14–17 January
- Lempert WR, Jiang N, Sethuram S, Samimy M (2002b) Molecular tagging velocimetry measurements in supersonic micro jets. *AIAA J* 40:1065–1070
- Miles RB, Grinstead J, Kohl RH, Diskin G (2000) The RELIEF flow tagging technique and its application in engine testing facilities and for helium–air mixing studies. *Meas Sci Technol* 11:1272–1281
- Pitz RW, Wehrmeyer JA, Ribarov LA, Oguss DA, Btlwala F, DeBarber PA, Deusch S, Dimotakis PE (2000) Unseeded molecular flow tagging in cold and hot flows using ozone and hydroxyl tagging velocimetry. *Meas Sci Technol* 11:1259–1271
- Stier B, Koochesfahani MM (1999) Molecular tagging velocimetry (MTV) measurements in gas phase flows. *Exp Fluids* 26:297–304
- Thurber MC, Grisch F, Kirby BJ, Votsmeier M, Hanson RK (1998) Measurements and modeling of acetone laser-induced fluorescence with implications for temperature-imaging diagnostics. *Appl Optics* 37:4963–4978